



# Single layer microwave absorber based on expanded graphite–novolac phenolic resin composite for X-band applications



Jyoti Prasad Gogoi<sup>a</sup>, Nidhi Saxena Bhattacharyya<sup>a,\*</sup>, Satyajib Bhattacharyya<sup>b</sup>

<sup>a</sup> Microwave Engineering Laboratory, Department of Physics, Tezpur University, Tezpur 784028, India

<sup>b</sup> Department of Electronics and Communication Engineering, Tezpur University, Tezpur 784028, India

## ARTICLE INFO

### Article history:

Received 15 May 2013

Received in revised form 26 September 2013

Accepted 25 October 2013

Available online 5 November 2013

### Keywords:

A. Particle-reinforcement

B. Electrical properties

D. Electron microscopy

Reflection loss measurement

## ABSTRACT

Expanded graphite–novolac phenolic resin (EG/NPR) composites in (5, 7, 8 and 10) wt.% of EG are developed as dielectric radar absorbing material in the X-band. Complex permittivity ( $\epsilon_r = \epsilon'_r - j\epsilon''_r$ ) of the composites measured in X-band are used to compute the reflection loss ( $RL_c$ ) of conductor backed single layer EG/NPR composites by optimizing the composites thickness ( $d$ ). Practical reflection loss measurements are carried out using free space technique. Impedance matching condition and quarter wavelength criteria are used for analysis of the reflection loss performance of the composites. The 5 wt.% EG/NPR composite shows measured reflection loss peak of value  $\sim -43$  dB at 12.4 GHz which is in close agreement with that of calculated reflection loss value  $\sim -53$  dB at the same frequency. The reflection loss peak shifts towards low frequency with increase in wt.% of EG and a  $-10$  dB absorption bandwidth  $\sim 1$  GHz is found for conductor backed single layer absorber with 7, 8 and 10 wt.% EG/NPR compositions.

© 2013 Elsevier Ltd. All rights reserved.

## 1. Introduction

Wireless technology stride towards gigahertz frequency applications in modern communication system has increased the electromagnetic interference (EMI), hindering the normal operation of the electronics systems. To control this ever increasing EMI pollution, the demand on efficient EMI shielding or radar absorbing materials (RAM) is increasing [1]. RAMs are functional materials that absorb microwave energy incident on it. Ideally, RAM should have minimum reflection and maximum attenuation of the microwave energy within the absorber matrix. The reflection phenomenon occurs mainly at two location; firstly at the air-absorber interface and secondly from the metal backing of the RAM. Reflection at the interface can be minimized by making input impedance of RAM close to that of free space. The input impedance at the air-RAM interface is determined from the expression,  $Z_{in} = Z_0 \sqrt{\mu_r/\epsilon_r} \tan[j(2\pi fd/c)\sqrt{\epsilon_r\mu_r}]$  where  $Z_0 = 377 \Omega$  [2]. The expression shows the dependence of  $Z_{in}$  on RAM material properties namely the complex permittivity,  $\epsilon_r (= \epsilon'_r - j\epsilon''_r)$ , complex permeability  $\mu_r (= \mu'_r - j\mu''_r)$ , and external parameters like the thickness,  $d$ , of the RAM and incident microwave frequency,  $f$  [3]. To realize impedance matching between the RAM and the free space interface, the ratio of  $\mu'_r/\epsilon'_r$  should approach to unity [4]. For a dielectric RAM,  $\mu_r = 1 - j.0$ , the intrinsic tunable parameter to achieve impedance

matching, is by making  $\epsilon'_r$  close to unity. Within the RAM, microwave energy decays exponentially with distance  $x$  by factor  $e^{-\alpha x}$  where attenuation constant ( $\alpha$ ) is given by [4]

$$\alpha = \frac{\sqrt{2}\pi f}{c} \times \sqrt{(\mu'_r\epsilon''_r - \mu''_r\epsilon'_r) + \sqrt{(\mu'_r\epsilon''_r - \mu''_r\epsilon'_r)^2 + (\epsilon'_r\mu'_r + \epsilon''_r\mu''_r)^2}}$$

The expression indicates that attenuation of microwave power for a dielectric absorber depends on  $\epsilon_r$ . An establish technique for increasing  $\epsilon_r$  is by adding electrically conducting metal particles in the polymer matrix, but has its own inherent drawbacks of being heavy weight, rigid and prone to corrode [5]. Practical applications require RAM structure to be lightweight and corrosion resistant apart from obtaining desired absorption with as thin as absorber structure. Carbon based materials such as carbon nanotubes; short carbon fibers etc. also show good microwave absorption which are comparatively lightweight and corrosion resistant [6–9]. However, processing complexities and high cost becomes a limitation for its commercial applications.

Expanded graphite (EG) flakes can be a promising filler material for RAM, with low weight (density  $\sim 0.005$ – $0.01$  g/cc), low cost of production, high electrical conductivity of  $\sim 10^4$  S/cm and is also resistant to environmental corrosion [10]. EG flakes are bi-dimensional carbon nanostructures consisting of small stacks of graphene sheets having thickness in the range from one to few tens of nanometers and the lateral linear dimensions varying from a few micrometers up to hundreds of micrometers [11].

The current authors in their previous work [12] reported high dielectric loss  $\epsilon''_r/\epsilon'_r > 1$  for 30, 40 and 50 wt.% EG – novolac phenolic

\* Corresponding author. Tel.: +91 (3712) 275551/275555; fax: +91 (3712) 267005/6.

E-mail address: [nidhisbhatta@gmail.com](mailto:nidhisbhatta@gmail.com) (N.S. Bhattacharyya).

resin (NPR) composites over the entire frequency range from 8.2 to 12.4 GHz which was indicative of the material being inherently highly lossy. However, subsequent reflection loss measurement with these composites showed poor reflection loss ( $\sim -3$  dB) properties. Further analysis of this poor performance reveals that although  $\epsilon_r''/\epsilon_r' > 1$ , the real permittivity  $\epsilon_r'$  by itself was as high as 5 which was far above the ideal value of 1 as dictated by the expression  $\mu_r''/\epsilon_r' = 1$ , to meet the condition of good impedance match for low reflection at the interface.

With a view to improve impedance matching at the surface, wt.% of EG, in the present investigation had been lowered in an effort to bring down the value of  $\epsilon_r'$ . The reason is that although the lossy part due to EG ( $\epsilon_r''$ ) will reduce the lowering of  $\epsilon_r'$  to a considerable extent will offset the reduction of the overall loss properties ( $\epsilon_r''/\epsilon_r'$ ) of the material. Hence a practical acceptable compromise is possible to be achieved between two conflicting conditions determining the overall performance of the RAM. The reflection loss of single layered EG–NPR composite for different compositions and thickness are computed using measured complex permittivity values. Absorption measurements are carried out using free space technique over the X-band. Results are analyzed using the measured complex permittivity values and corresponding computed impedances.

## 2. Experimental

### 2.1. Preparation of EG–NPR composites

EG–NPR composites are prepared using mechanical mixing and thermal treatment method. Initially, EG flakes are synthesized by heating graphite intercalated compound (GIC) at  $\sim 900^\circ\text{C}$  [12]. The EG flakes are mechanically mixed with NPR powder in 5, 7, 8 and 10 wt.% of EG. The samples are molded to different dimensions as per the requirement, by heating the EG–NPR mixture at  $\sim 150^\circ\text{C}$  under a pressure of  $\sim 2$  tons. Both, EG/NPR composite and EG are characterized for its crystalline structure, size and distribution using XRD, TEM and SEM respectively. XRD is carried out using Rigaku Miniflex 200 with monochromatic Cu K $\alpha$  radiation ( $\lambda = 1.54178 \text{ \AA}$ ) over  $2\theta$  angle from  $10^\circ$  to  $70^\circ$ . Surface morphology and growth structure of EG is studied by scanning electron microscope (SEM)–JEOL JSM-6390LV. Transmission electron microscopy is carried out using JEOL JEM-2100, operating at an accelerating voltage of 200 kV. In-plane dc electrical conductivity of the composites is measured by two probe method using Keithley 2400C – source meter.

### 2.2. Microwave characterization techniques

Samples of dimension  $10.38 \text{ mm} \times 22.94 \text{ mm} \times 3 \text{ mm}$  is used for X band characterization. Scattering parameters ( $S_{11}$  and  $S_{21}$ ) are measured by Transmission/Reflection method using Agilent WR-90 X11644A rectangular waveguide line compatible with Agilent E8362C vector network analyzer and complex permittivity are determined from measured  $S_{11}$  and  $S_{21}$  using Nicolson–Ross method [13] with an in-house developed MATLAB program.

### 2.3. Free space absorption measurements

The microwave-absorption characteristics are evaluated by measuring the reflection loss ( $RL_m$ ) using Agilent E8362C vector network analyzer in the frequency range of 8.2–12.4 GHz. Prior to  $RL_m$  measurements, the system is calibrated using Through-Reflect-Line (TRL) method [14]. A pair of spot focusing plano-convex lens is used to reduce the required dimension of the test sample.

For  $S_{11}$  measurements the dimension of the reference metal sheet is kept the same as the RAM dimension.

## 3. Results and discussions

### 3.1. Microstructural and dc electrical conductivity studies

Room temperature X-ray patterns of NPR, NG, EG and EG/NPR composite are shown in Fig. 1. A broad peak at about  $20^\circ$  is observed for NPR confirming its amorphous characteristic (Fig. 1(a)). The  $d$ -spacing of the graphite flakes is calculated using the Bragg's Equation [15]. Fig. 1(b) shows the characteristic (002) peak of NG at  $2\theta = 26.86^\circ$  corresponding to inter-layer spacing ( $d_{002}$ ) 0.332 nm, confirming its crystalline nature. EG characteristic peak is observed at slightly lower angle than NG at  $2\theta = 26.62^\circ$ , corresponding to inter-layer spacing ( $d_{002}$ ) 0.335 nm, as seen from Fig. 1(c). The calculated microstrain ( $\chi$ ) determined by single line approximation method [16] is found to be 0.7% for NG which increases upto 1.36% for EG. The increase in the microstrain and  $d$  spacing confirms the formation of EG. XRD of EG/NPR composite shows sharp reflection at  $2\theta = 26.62^\circ$ , as observed in Fig. 1(d), implying that graphite nanosheets in the composite has the same  $d$  spacing as that of EG confirming that the crystalline structure of EG is retained in the composite. Surface morphology of EG flakes, as seen in SEM micrograph in Fig. 2(a), reveals numerous graphite sheets in EG of thickness in nanometer range and lateral dimension in few micrometers. The thickness of EG sheet is confirmed in TEM micrograph and is found to be 10–40 nm and the lateral length of about 400 nm (Fig. 2(b)) indicating a large aspect ratio (width-to-thickness), which facilitates the conductive network.

The in-plane dc conductivity ( $\sigma$ ) of EG/NPR composites as a function of EG mass fraction ( $p$ ) measured at room temperature is tabulated in Table 1. It is seen that the electrical conductivity increases with EG loadings. The composites developed, consist of insulating phenolic resin phase ( $\sim 10^{-11} \text{ S/cm}$ ) and conducting EG flakes ( $\sim 10^4 \text{ S/cm}$ ). Pure NPR shows insulating behavior, however, inclusion of EG loadings ( $\sim 5$  wt.%) transform the insulating composites to semiconducting state thus establishing a conductive

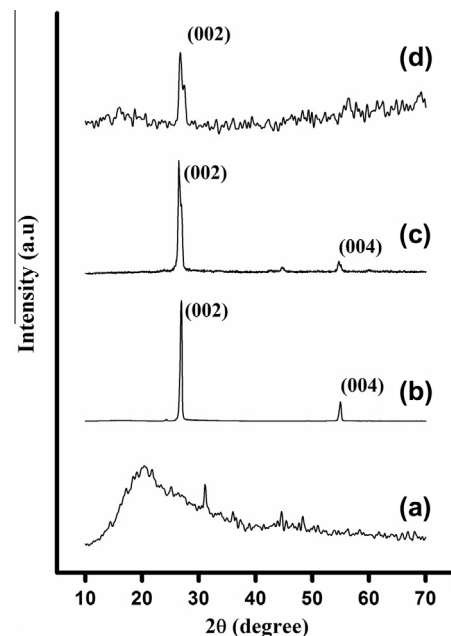


Fig. 1. XRD patterns of (a) NPR, (b) NG, (c) EG and (d) EG/NPR composite.

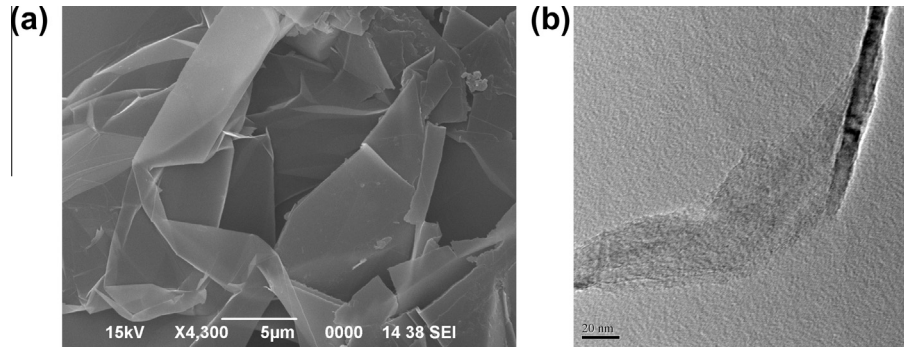


Fig. 2. (a) SEM micrograph of EG and (b) TEM micrograph of EG.

Table 1

DC electrical conductivity ( $\sigma$ ) of EG/NPR composites with varying wt.% of EG.

EG mass fraction (p)	0 wt.%	5 wt.%	7 wt.%	8 wt.%	10 wt.%
dc Conductivity ( $\sigma$ ) (S/cm)	2.4E-11	6.05E -07	3.96E-06	9.88E-06	4.78E-05

network of EG in the composite system and enhancing its electrical conductivity.

### 3.2. Dielectric properties

Fig. 3(a) and (b) shows the real  $\epsilon_r'$  and imaginary  $\epsilon_r''$  parts of complex permittivity, respectively, measured for NPR and EG/NPR composites over the X-band. The  $\epsilon_r'$  and  $\epsilon_r''$  values of NPR shows a constant value of  $\sim 2.5$  and  $\sim 0.6$ , respectively over the X-band. The  $\epsilon_r'$  values for 5 wt.% lie from 4.7 at 8.2 GHz to  $\sim 2$  at 12.4 GHz, i.e. decreasing trend with increase in frequency.  $\epsilon_r'$  spectra for 7, 8 and 10 wt.% composites shows an increasing trend with increase in EG percentages in the composites with maximum values ranging from 8.6 at 8.2 GHz to 7.7 at 12.4 GHz for 10 wt.% composition. These compositions also show a decreasing trend with increasing frequency. The  $\epsilon_r''$  spectra for 5 wt.% shows almost a constant value of  $\sim 1.0$  till 11.5 GHz and at 12.4 GHz a resonance peak is observed with  $\epsilon_r'' = 1.9$ . With increase in the EG wt.%, the values of  $\epsilon_r''$  increases and the resonance peak values of 1.9, 2.07, 2.5 and 3.42 are observed at 12.4, 12.0, 11.16 and 9.7 GHz for 5, 7, 8 and 10 wt.% composites, respectively. Since the EG/NPR composite is a heterogeneous system consisting of conducting EG flakes and insulating NPR, the interfacial polarization leads to the loss mechanism due to the associated relaxation phenomenon. EG flakes have  $\pi$ -electrons that can travel freely within the flakes and accumulate at the EG–NPR interface, forming a structure similar to a boundary-layer capacitor which generates the interfacial electric dipolar polarization [17], which may increase the loss.

### 3.3. Attenuation constant

The attenuation constant ( $\alpha$ ) of the NPR and EG/NPR composites calculated from measured complex permittivity in X-band is shown in Fig. 4. It is seen that the value of  $\alpha$  increases for higher EG loadings. Increase in attenuation can be attributed to conduction loss; dielectric relaxation and interfacial polarization [18,19]. Conduction loss is due to directional motion of charge carriers and is dependent on composites conductivity. Dielectric relaxation occurs because of the orientation polarization of intrinsic dipoles. Presence of conducting EG in insulating NPR produce interfacial polarization. Higher percentages of EG increase these properties and consequently attenuation increases. It is also observed that a

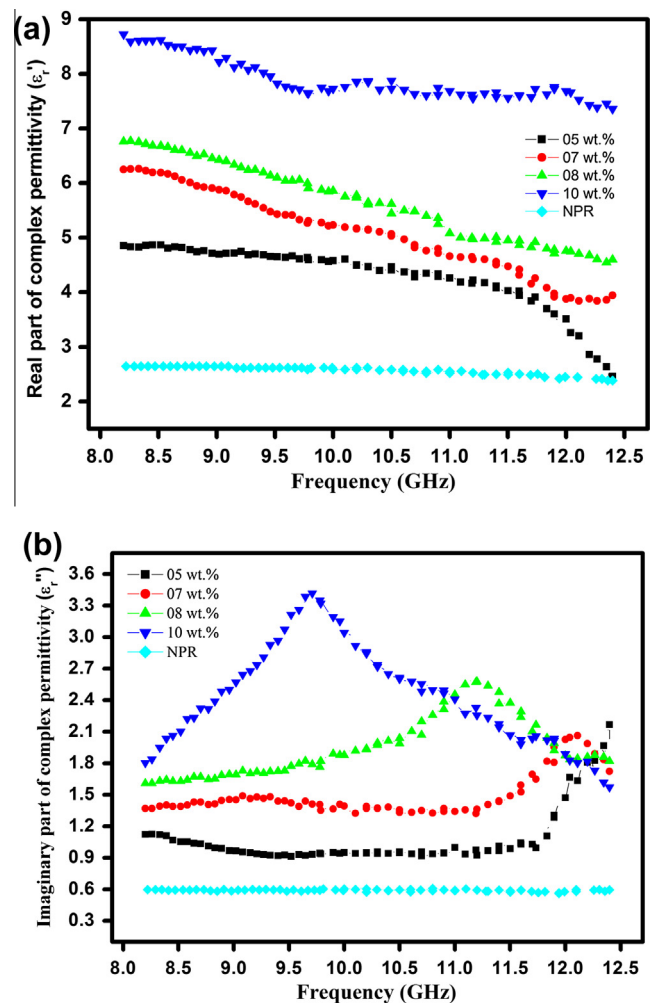


Fig. 3. Complex permittivity of EG/NPR composite (a) real permittivity and (b) imaginary permittivity.

maximum value of attenuation is achieved for 5 wt.%, 7 wt.%, 8 wt.% and 10 wt.% EG/NPR composites at 12.4, 12, 11 and 9.5 GHz respectively.

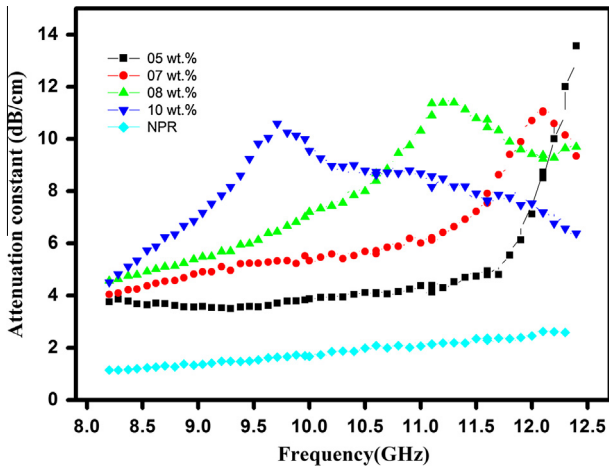


Fig. 4. Attenuation constant values of EG/NPR composites.

3.4. Microwave absorbing properties

The reflection loss,  $RL_c$  (dB), of a single-layer material backed with perfect conductor is determined using transmission line theory [2,20], given by

$$RL_c = 20 \log \left| \frac{Z_{in} - Z_0}{Z_{in} + Z_0} \right| \quad (1)$$

$$RL_c = 20 \log \left| \frac{\sqrt{\mu_r/\epsilon_r} \tanh(j2\pi f/c) \sqrt{\mu_r \epsilon_r} d - 1}{\sqrt{\mu_r/\epsilon_r} \tanh(j2\pi f/c) \sqrt{\mu_r \epsilon_r} d + 1} \right| \quad (2)$$

Complex permeability measurements of EG–NPR composites show a nonmagnetic characteristic i.e.  $\mu' = 1$  and  $\mu'' = 0$ .  $RL_c$  values, as seen from Eqs. (1) and (2), depend on material parameter  $\epsilon'$  and  $\epsilon''$  and also on the thickness,  $d$ , of the EG–NPR composite. The RAM is developed for strategic defense applications, where for most applications the desired thickness is about 4 mm [21]. Hence,  $RL_c$  values are determined with thickness variation of  $d = 2, 4$  and  $6$  mm for all the composites over the X-band. As compared to 2 mm and 6 mm thickness, sample of 4 mm shows good  $RL_c$  over the test frequency range as seen from Fig. 5. An  $RL_c \sim -53$  dB for 5 wt.% composition at 12.4 GHz for 4 mm thick sample (Fig. 5(b)) is observed. The absorption peaks show a shift towards the lower

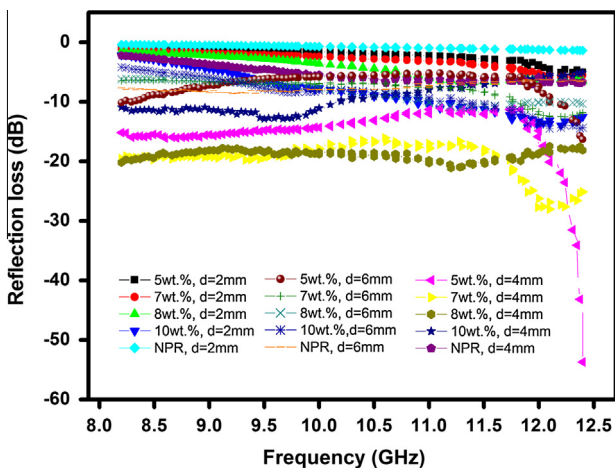


Fig. 5. Calculated reflection loss of EG/NPR composites for (a) 2 mm, (b) 4 mm and (c) 6 mm thickness.

frequency and  $RL_c$  decreases as EG concentration in the composite increases. 7 wt%, 8 wt% and 10 wt% EG composite shows a maximum reflection loss of  $-27$  dB,  $-20$  dB and  $-10$  dB with peaks at 12 GHz, 11 GHz and 9.5 GHz, respectively.

Based on the computed  $RL_c$  in the above paragraph, a conductor backed single layer RAM of 4 mm thickness is designed and tested for microwave absorption over the X band. A schematic representation of free space reflection loss measurement system is shown in Fig. 6. The microwave power is incident on the sample with dimension of  $152 \text{ mm} \times 152 \text{ mm} \times 4 \text{ mm}$ . The incident wave is partly reflected from the interface surface and partly absorbed [22]. If  $P_{in}$  is the incident power density on the sample,  $P_R$  is the reflected power density and  $P_A$  is the absorbed power by the test sample, then

$$P_{in} = P_R + P_A \quad (3)$$

$RL_m$  and  $A$ , are the measured reflection loss and the absorption loss in decibels (dB), respectively, and given as

$$RL_m = 10 \log P_R/P_{in} \quad (4)$$

$$A = 10 \log P_A/P_{in} \quad (5)$$

Here,  $RL_m$  is a measure of the microwave-absorbing efficiency. Fig. 7 shows the experimental results of  $RL_m$  for the EG/NPR composites in 8.4–12.4 GHz range. The composite with 5 wt.% EG shows maximum  $RL_m \sim -43$  dB while the calculated  $RL$  is  $-53$  dB both being at 12.4 GHz which is in general agreement in terms of order of magnitude even though the values are not in close agreement. With increasing EG wt.% in the composite, the absorption peak shifts towards the lower end of X-band with reduced wave absorption ability. The  $RL_m$  values of  $-20$  dB,  $-16$  dB and  $-12$  dB are observed for 7 wt.%, 8 wt.% and 10 wt.% EG with absorption peak at 12 GHz, 10.42 GHz and 9.75 GHz respectively, a trend found to be as predicted by theory. A maximal microwave absorption occurs at matching thickness,  $d_m$ , when  $d_m$  equals to an odd multiple of  $\lambda_m/4$  (where  $\lambda_m = \lambda_0/(|\epsilon_r||\mu_r|)^{1/2}$ ), the condition for phase cancellation [23]. For 5 wt.% composite at 12.4 GHz,  $d_m = 3.6$  mm which is near to 4 mm and hence shows the highest reflection loss at that frequency (Fig. 7). The  $d_m$  for 7, 8 and 10 wt.% composites is 3.2 mm, 3 mm and 2.8 mm at  $\sim 12$  GHz, 11 GHz and 9.2 GHz respectively, which deviates more from the actual thickness of 4 mm which explains the poor measured  $RL_m$  performance. According to Eq. (2), minimum reflection will take place when real input impedance,  $Z'_{in}$  approaches  $377 \Omega$  and the corresponding imaginary input impedance,  $Z''_{in}$ , approaches zero  $\Omega$  [24]. It is seen from Fig. 8(a and b) that at 12.4 GHz,  $Z'_{in}$  and  $Z''_{in}$  for 5 wt.% composite are found to be  $375 \Omega$  and  $75 \Omega$  respectively which is the closest to the required values of  $377 \Omega$  and zero  $\Omega$ . Hence the best imaginary matching is observed at 12.4 GHz with  $RL_m$  of  $-43$  dB for this composition. From Fig. 3, it is seen that for 5 wt.% EG/NPR composites,  $\epsilon'_r$  is closest to the required matching condition with a value of 2.35 at 12.4 GHz, the case for which the best overall  $RL_m$  performance is

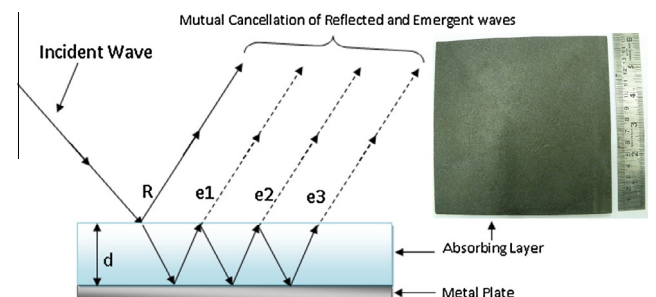


Fig. 6. Schematic representation of microwave absorption measurement.

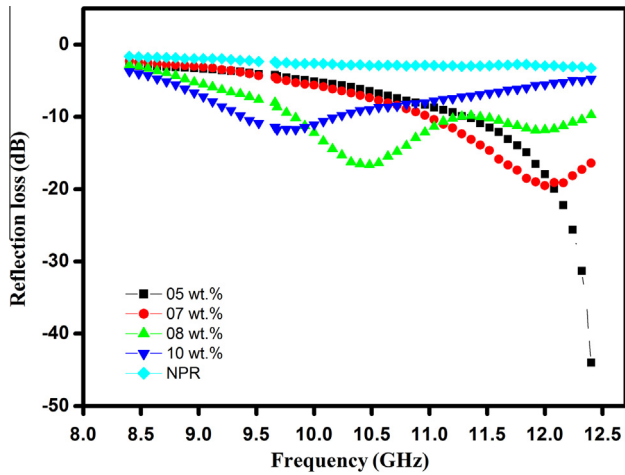


Fig. 7. Measured reflection loss of EG/NPR composites of 4 mm thickness.

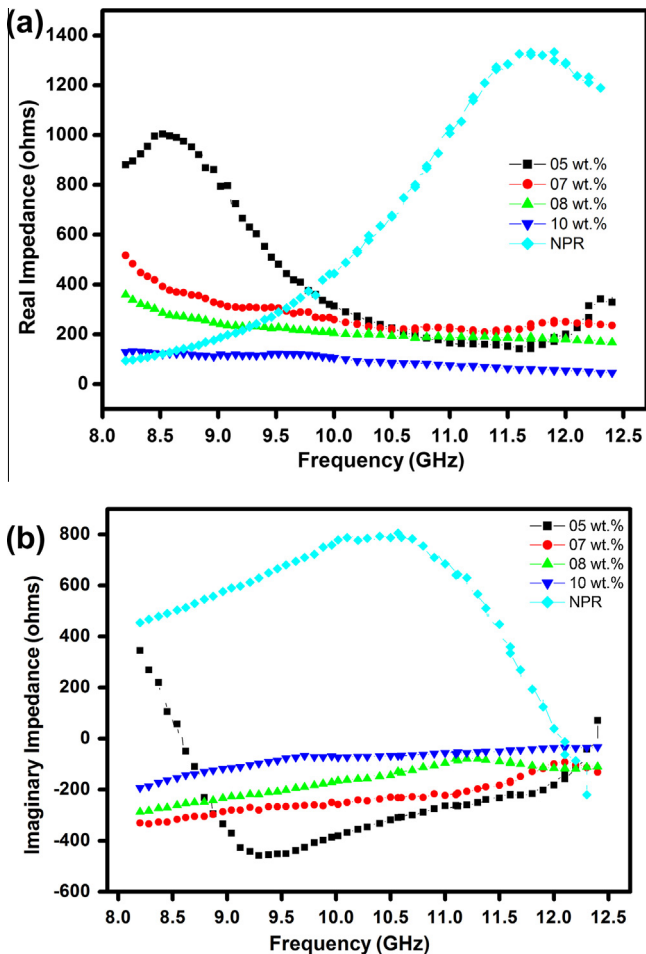


Fig. 8. Complex impedance of 4 mm EG/NPR composites (a) real impedance and (b) imaginary impedance.

observed. This result is a fair indication of the dominant role of impedance matching on the overall absorption performance of the developed absorbers. It may be mentioned that a wide bandwidth absorption of at least  $-10$  dB is obtained (Fig. 8) for 7 wt.%, 8 wt.% and 10 wt.% in the frequency ranges of 11.0–12.4 GHz, 9.8–11.2 GHz and 9.3–10.1 GHz respectively. Hence, for a dielectric microwave absorber with small thickness of 4 mm, a wide

absorption bandwidth can be obtained over different frequency ranges. This offers the option to the designer to simply vary the wt.% of EG to tune the absorption to a desired frequency range in applications where thickness cannot be increased and absorption performance requirement is not too stringent. Moreover, the weight of fabricated EG/NPR composites tiles of dimension  $152 \text{ mm} \times 152 \text{ mm} \times 4 \text{ mm}$  is found to be 68.9 grams with negligible water absorption percentages of 0.08. The microwave absorber, thus fabricated from EG/NPR composites can be used on plane structure subjected to X-band frequencies radiation in both indoor as well as outdoor environment efficiently.

#### 4. Conclusions

Composites with low wt.% of EG have been developed and their absorption performance is evaluated. The results had been analyzed using  $\epsilon'_r$ ,  $\epsilon''_r$  values and the corresponding impedances. Results of the developed composites indicates that for all the different composites (5, 7, 8 and 10 wt.% EG), a wide bandwidth of  $-10$  dB absorption can be obtained in the X-band frequency range. Moreover, the absorption frequency ranges can be shifted by nearly changing the wt.% of EG even while keeping the thickness constant at 4 mm which is less than some of the low thickness industrial standard dielectric absorbers. The developed EG/NPR composites being light weight, environmentally resistant and low fabrication cost makes it ideal for used in applications such as weather radars operating in frequency range 9.3–9.5 GHz, in precision approach radar (PAR) works at 9.0–9.2 GHz, etc.

#### Acknowledgement

The authors would like to sincerely thank Department of Information Technology, New Delhi for providing financial support.

#### References

- [1] Jalalia M, Dauterstedt S, Michaud A, Wuthrich R. Electromagnetic shielding of polymer-matrix composites with metallic nanoparticles. *Compos Part B Eng* 2011;42:1420–6.
- [2] Srivastava RK, Narayanan TN, Mary RAP, Anantharaman MR, Srivastava A, Vajtai R, et al. Ni filled flexible multi-walled carbon nanotube-polystyrene composite films as efficient microwave absorbers. *Appl Phys Lett* 2011;99:113116.
- [3] Michielssen E, Sajer J, Ranjithan S, Mitra R. Design of lightweight, broad-band microwave absorbers using genetic algorithms. *IEEE T Microw Theory* 1993;41:1024–30.
- [4] Zhang B, Yong F, Xiong J, Yang Y, Lu H. Microwave absorbing properties of de-aggregated flake shaped carbonyl iron particle composites at 2–18 GHz. *IEEE T Magn* 2006;42:1778–81.
- [5] Goyal RK, Kadam A. Polyphenylene sulphide/graphite composites for EMI shielding applications. *Adv Mater Lett* 2010;1(2):143–7.
- [6] Yonglai Y, Gupta MC, Dudley KL, Lawrence RW. Novel carbon nanotube-polystyrene foam composites for electromagnetic interference shielding. *Nano Lett* 2005;5:2131–4.
- [7] Liu Z, Bai G, Huang Y, Ma Y, Du F, Li F, et al. Reflection and absorption contributions to the electromagnetic interference shielding of single-walled carbon nanotube/polyurethane composites. *Carbon* 2007;45:821–7.
- [8] De Rosa IM, Dinescu A, Sarasini F, Sarto MS, Tamburrano A. Effect of short carbon fibers and MWCNTs on microwave absorbing properties of polyester composites containing nickel-coated carbon fibers. *Compos Sci Technol* 2010;70:102–9.
- [9] Liu X, Zhang Z, Wu Y. Absorption properties of carbon black/silicon carbide microwave absorbers. *Compos Part B Eng* 2011;42:326–9.
- [10] Eui LS, Oyoung C, Hahn HT. Microwave properties of graphite nanoplatelet/epoxy composites. *J Appl Phys* 2008;104:033705-1–5-7.
- [11] Du X, Skachko I, Barker A, Andrei EY. Approaching ballistic transport in suspended graphene. *Nat Nanotechnol* 2008;3:491–5.
- [12] Gogoi JP, Bhattacharyya NS, Raju KCJ. Synthesis and microwave characterization of expanded graphite/novolac phenolic resin composite for microwave absorber applications. *Compos Part B Eng* 2011;42:1291–7.
- [13] Nicolson AM, Ross GF. Measurement of the intrinsic properties of materials by time-domain techniques. *IEEE T Instrum Meas* 1970;IM-19:377–82.
- [14] Ghodgaonkar DK, Varadan VV, Varadan VK. A free-space method for measurement of dielectric constants and loss tangents at microwave frequencies. *IEEE T Instrum Meas* 1989;37:789–93.

- [15] Cullity BD. Elements of X-ray diffraction. Addison Wesley; 1978.
- [16] Delhez R, Keijser THD, Langford JI, Louer D, Mittemeijer EJ, Young RA, editors. The reitveld method. Oxford: Oxford University press; 1956.
- [17] Zhang XF, Guan PF, Dong XL. Multidielectric polarizations in the core/shell Co/graphite nanoparticles. Appl Phys Lett 2010;96:223111.
- [18] Paton KR, Windle AH. Efficient microwave energy absorption by carbon nanotubes. Carbon 2008;46:1935–41.
- [19] Duan Y, Liu S, Wen B, Guan H, Wang G. A discrete slab absorber: absorption efficiency and theory analysis. J Compos Mater 2006;40:1841.
- [20] Li W, Zhu L, Gu J, Liu H. Microwave absorption properties of fabric coated absorbing material using modified carbonyl iron powder. Compos Part B Eng 2011;42:626–30.
- [21] Feng YB, Qiu T, Shen CY. Absorbing properties and structural design of microwave absorbers based on carbonyl iron and barium ferrite. J Magn Magn M 2007;318:8–13.
- [22] Fan ZJ, Luo GH, Zhang ZF, Zhou L, Wei F. Electromagnetic and microwave absorbing properties of multi-walled carbon nanotubes/polymer composites. Mater Sci Eng B 2006;132:85–9.
- [23] Zhang L, Zhu H, Song Y, Zhang Y, Huang Y. The electromagnetic characteristics and absorbing properties of multi-walled carbon nanotubes filled with Er<sub>2</sub>O<sub>3</sub> nanoparticles as microwave absorbers. Mater Sci Eng B 2008;153:78–82.
- [24] Micheli D, Apollo C, Pastore R, Marchetti M. X-Band microwave characterization of carbon-based nanocomposite material, absorption capability comparison and RAS design simulation. Compos Sci Technol 2010;70:400–9.